INVESTIGATION AND MITIGATION OF A FAILURE AT THE TAXIARCHES CANAL OF MORNOS AQUEDUCT

Mourtzas N.D.[1], Gkiolas A.[2], Vakiris D.[2] and Soulis V.[3]

[1]GAIAERGON Ltd, 16-18 Kefallinias Str., 152 31 Chalandri, Athens, gaiaergon@gmail.com

[2] GEOMECHANIKI S.A., 91 Eth. Antistaseos Str., 15351 Pallini, Athens, geomsot@gmail.com

[3] EYDAP S.A., Directory of Water Intake,16 Galatsiou Str., 1114, Athens, vsoulis@eydap.gr

Abstract

The sudden soil fracture and failure at the Taxiarches canal of Mornos Aqueduct of the Athens Water Supply and Sewerage Company (EYDAP SA), took place approximately 540m after the exit of Elikonas tunnel and resulted in failure and displacement of the canal segments along an 80m long section. Due to the failure the water supply was interrupted and two extensive gullies, spaced 75m apart, were created by the water outflow. The water discharge resulted in subsoil erosion and transportation of vast masses of geomaterial and two of the canal segments downhill. The debris flow destroyed part of Prodromos-Saranti Road, swapping along olive cultivations and causing extensive damage to Saranti settlement. The failure of the canal occurred in an area of steep morphology, at the front of an overthrust, within tectonic breccia and calcareous-clayey material of chaotic structure and reduced mechanical properties, vulnerable to erosion. The boundaries of the main fracture were defined by the thrust geometry.
The study of permanent remedial measures included excavation of a cut in the natural slope on the uphill side of the failure, construction of a bypass pipe founded on bedrock and of an anchored pile wall with pre-stressed anchors on the downhill side of the new pipe, excavation and removal of the temporary fill and finally construction of a reinforced fill for rehabilitation of the slide area.
Key words: *debris flow, soil fracture, overthrust, reinforced fill, rehabilitation.*

Περίληψη

Η αιφνίδια αστοχία του υπεδάφους έδρασης της Διώρυγας Ταξιαρχών του Υδαταγωγού του Μόρνου (Ε.ΥΔ.ΑΠ. Α.Ε.), σε απόσταση 540m μετά την έξοδό της από τη σήραγγα Ελικώνα, προκάλεσε τη θραύση και μετακίνηση των φατνωμάτων της, σε μήκος 80 m. Αποτέλεσμα της αστοχίας ήταν η προσωρινή διακοπή της υδροδότησης και η δημιουργία δύο εκτεταμένων μισγαγγειών, σε απόσταση 75 m μεταξύ τους, που διαμορφώθηκαν από την ορμή του διαφυγόντος νερού. Ο όγκος του νερού που διέφυγε μετέφερε τεράστιες μάζες γεωυλικών (λασπορροή) και δύο εκ των φατνωμάτων της διώρυγας. Από την αστοχία καταστράφηκε τμήμα του επαρχιακού δρόμου Πρόδρομου-Σαράντι, αποξηλώθηκαν ελαιοκαλλιέργειες και κατακλύστηκε σημαντικό τμήμα του οικισμού Σαράντι. Η αστοχία της διώρυγας εκδηλώθηκε σε περιοχή απότομου μορφολογικά ανάγλυφου, στην κεφαλή του μετώπου επώθησης και σε θέση όπου επικρατούν τεκτονικά λατυποπαγή, χαοτικής δομής ασβεσταργιλικά υλικά, τεκτονικά καταπονημένα, ευκολοδιάβρωτα και με μειωμένα μηχανικά χαρακτηριστικά. Τα όρια

της κύριας ολίσθησης καθορίζονται από τη γεωμετρία της επώθησης. Η μελέτη μόνιμης αποκατάστασης της υδροδότησης, περιελάμβανε την εκσκαφή ορύγματος στο φυσικό πρανές ανάντη της ολίσθησης, την κατασκευή νέου αγωγού εδραζομένου επί του βραχώδους υποβάθρου και πασσαλότοιχου με προεντεταμένα αγκύρια κατάντη του νέου αγωγού και τέλος εκσκαφή και απομάκρυνση της προσωρινής επίχωσης και κατασκευή οπλισμένου επιχώματος αποκατάστασης.

Λέξεις κλειδιά: εδαφική θραύση, λασπορροή, επώθηση, οπλισμένο επίχωμα, Αποκατάσταση.

1. Introduction

Debris flows are fast moving, liquefied landslides of unconsolidated mixtures of water and debris. They are common in sparsely vegetated steeplands throughout the world (Berti et al., 1999; Cannon et al., 2001a; Cannon et al., 2001b; Cannon et al., 2003; Godt and Coe, 2007; McArdell et al., 2007; Coe et al., 2008; Santi et al., 2008). Flows can carry material ranging in size from clay to boulders, and may contain a large amount of woody debris such as logs and tree stumps. Debris flows and landslides may lead to large-scale natural hazards, and may contribute to a large fraction of long-term sediment yields from mountain areas (Dadson et al., 2004). It is widely recognized that hillslope instability can be caused by increased subsurface pore pressures during periods of intense rainfall (Anderson and Sitar, 1995; Iverson et al., 1997), which reduce the shear strength of hillslope materials (Keefer, 1984). Relative to flows that initiate from a discrete landslide source, the mechanisms that contribute to the initiation and propagation of debris flows produced during runoff events are less understood (Cannon et al., 2003; Berti and Simoni, 2005; Coe et al., 2008; McCoy et al., 2010). Although hillslopes provide an important source of material, it has been recognized that a significant portion of the debris-flow volume is generated by erosion of channel fill (Cenderelli and Kite, 1998; Bovis and Jakob, 1999; Jakob et al., 2005; Santi et al., 2008). Mobilization of material stored in the channel can be considered to be the product of shear forces applied on the bed by the flow, impulsive loading, liquefaction of channel fill, bank failure, and headward migration of knickpoints (Bovis and Dagg, 1992; Egashira et al., 2001; Hungr et al., 2005). Channel deposition will occur when friction increases along flow margins and internal pore-fluid pressures diminish (Major, 2000).

The soil failure at the Taxiarches Canal, on the southern outskirts of the mountainous mass of Elikonas, around 3 km West and North of the settlements of Prodromos and Saranti in Thiva region 540m after the exit of Elikonas tunnel, caused fracture and movement of its segments (Figure 1). Due to the canal segments failure, Athens' water supply was temporary interrupted and large amounts of water flowed out, causing sudden erosion and massive displacement of soil material. Two extended gullies formed throughout the steep slope and downhill to the Spartia streams's riverbed, flooding it with debris. Part of the Road connecting Saranti and Prodromos settlements were destroyed. Olive cultivations swept along and a significant part of Saranti settlement, mainly houses near the sea, flooded. In the greater area of the landslide, a significant number of soil movements and canal failures have been recorded in the past, during the earthquake of 1981 but also within the following years (Leonards et al., 1993).

2. Description of the Failure

In the afternoon of 29/03/2011 a significant soil fracture and failure at the Taxiarches canal of Mornos Aqueduct took place, extending to a section of approximately 7 canal segments, with an 11.50 m to 12 m length each (total length 80 m).

The reinforced concrete canal cross-section is U-shaped with a width of 5 m and 4.50 m height. The canal is constructed in cut and its hillside wall was backfilled up to a 4m height, where a surveillance road is allocated. Due to the failure, two of the canal segments (No 6 and 7) slid

downhill and four segments upstream (2, 3, 4 and 5) and another one downstream (8) tilted and were damaged (Figures 1 and 2). During the final phase of the failure, water discharge dropped from 100 m³/sec to 10 m³/sec, within a two to three minutes time period, resulting in an estimated outflow volume in the order of 300 to 400 thousand cubic meters. This sudden outflow resulted in erosion of 45.000 m³ soil material, consisting of fine and coarse grained material of the overthrust zone.

Figure 1 - Aerial view of the slide area.

At the area of the slid segments, the subsoil, the surveillance road and part of the cut slope have also slid downhill forming a gully (eastern) with steep high sides, with a length of 150 m, a maximum width of 45 m and depth ranging between 10 m to18 m. Upstream the main failure area, four canal segments have undergone significant displacements, mainly horizontal towards lower elevations. At the area of the most distant segment a secondary gully (western gully) with steep sides was formed, with a length of 250 m, a maximum width of 18 m and depth ranging from 2 m to3 m (Figures 1 and 2).

Figure 2 - Canal segment failure (left), Main slide shortly after occurrence (right).

Immediate remedial measures were taken, including temporary filling of part of the failed and eroded soil mass and construction of temporary twin bypass pipes, of 2 m diameter each. Backfilling for the pipes foundation was implemented by means of a steep temporary embankment, using material from a nearby quarry, without proper compaction.

3. Morphological Features of the Landslide Area

The landslide area is located at the SW outskirts of an extended morphological range, with an axis of NW-SE direction, and defined by the two main hydrographic features of the greater area, the streams of Taxiarchis at the East and Spartia at the West, which converge at its lower end, downhill the slide, forming the Saranti stream (Figure 1).

The sudden discharge of a great water volume, after the canal failure, created two gullies spaced 75 m apart. The eastern major gully, of a length of 150 m, has a direction of NNW-SSE, maximum width of 45 m and it is 18 m deep (Figures 1 and 3). Its slopes are steep with gradients reaching 80% in the western slope, where friable and vulnerable to erosion calcareous-clayey materials are predominant and 100% in the eastern, where sandstones and conglomerates are developed.

The morphological gradients of the relatively steep riverbed can be divided into three sections, which are separated by two scarps, with heights of 9m and 5m, respectively. The first scarp is located in a distance of 70 m from the canal level and the second in a distance of 103 m. The gradients reach 70% in the first section, 37% in the second and 57% in the lower one (Figures 1, 3 and 4).

The western and smaller size gully has a direction of NE-SW, a length of 110 m, a maximum width of 17 m and it is 8 m deep, due to less volume of discharge. The inclinations of its eroded sides are in the order of 100% at the western and 65% at the eastern side slope, while the mean longitudinal gradient of the gully is 65% (Figures 1, 3 and 4).

4. Geology of the Landslide Area

The greater landslide area is characterized by geological formations of the Parnassos – Giona unit and by sediments of the Subpelagonic zone (Papastamatiou et al., 1971; Papanikolaou, 1986). The boundaries of the unstable mass coincide with the overthrust zone of Cenomanian and Upper Triassic flysch formations of the Subpelagonic unit, overlying the Palaeogene flysch of the Parnassos-Giona unit. The intense tectonic deformation of flysch materials, has favoured the formation of a zone with poor mechanical properties, which coincides with the slid section of the unstable mass.

The flysch formations of the Parnassos-Giona unit comprise the massive bedrock of the landslide area (Figures 3 and 4). The conglomerates of this unit show a high degree of diagenesis and consist of schist, quartz, chert and limestone gravels and cobbles, with a particle size ranging from 0.01 m to 0.10 m, within a quartz, siliceous or carbonic matrix. Sandstone layers consisting of coarse-grained, ash-green coloured, massive sandstone crossed by quartz veins as well as lenticular intercalations of limestones, are interpolated. The green to ash-green coloured schists, with white quartz veins, present an intense microfolding as well as fragmentation and detachment along the schistosity planes.

Due to its intense tectonic deformation the Cenomanian overthrusted flysch system is a mélange without a specific stratigraphic meaning in the wider area. It is comprised of sandstones, purple coloured clayey schists and mudstones and coarse fragments and limestone blocks. It has been eroded and removed from the failure area. Calcareous relics of the Subpelagonic unit are also located uphill and downhill of the failure area. Tectonic materials lie above the overthrust surface and have a total thickness of ca. 15 m. They consist of intensively fragmented sandstones and conglomerates, clays with cobbles and gravels and calcareous-clayey foliaceous soils. Finally, scree and eluvial flysch deposits are the youngest formations of the landslide area.

According to the geological mapping of the failure area (Figures 3 and 4), schists with intercalations of thinly and thickly bedded sandstones are located at the base of the stratigraphic sequence. At their southern boundary show a general dip towards the south (ranging from SE to SW) at angles 50° to 80°. At their northern appearances are dipping towards NNE and NNW at

angles 35° to 40°. The extended limestone body, massive to thickly bedded, with a general dip to NE at angle 20°, follows. The next formation uphill are alternations of thinly to thickly bedded sandstones with a limited schist intercalation, dipping 25° to 35° NE, with thickness of ca.35 m. They are followed by cohesive and massive conglomerates. Tectonic breccia covers the tectonic surfaces. The ash-green coloured schists with limestone intercalations are located at the foot of the western gully, dipping 10° WNW. Thickly and thinly bedded, intensively tectonized sandstones follow, dipping 70° to 75° SW (Figures 3 and 4).
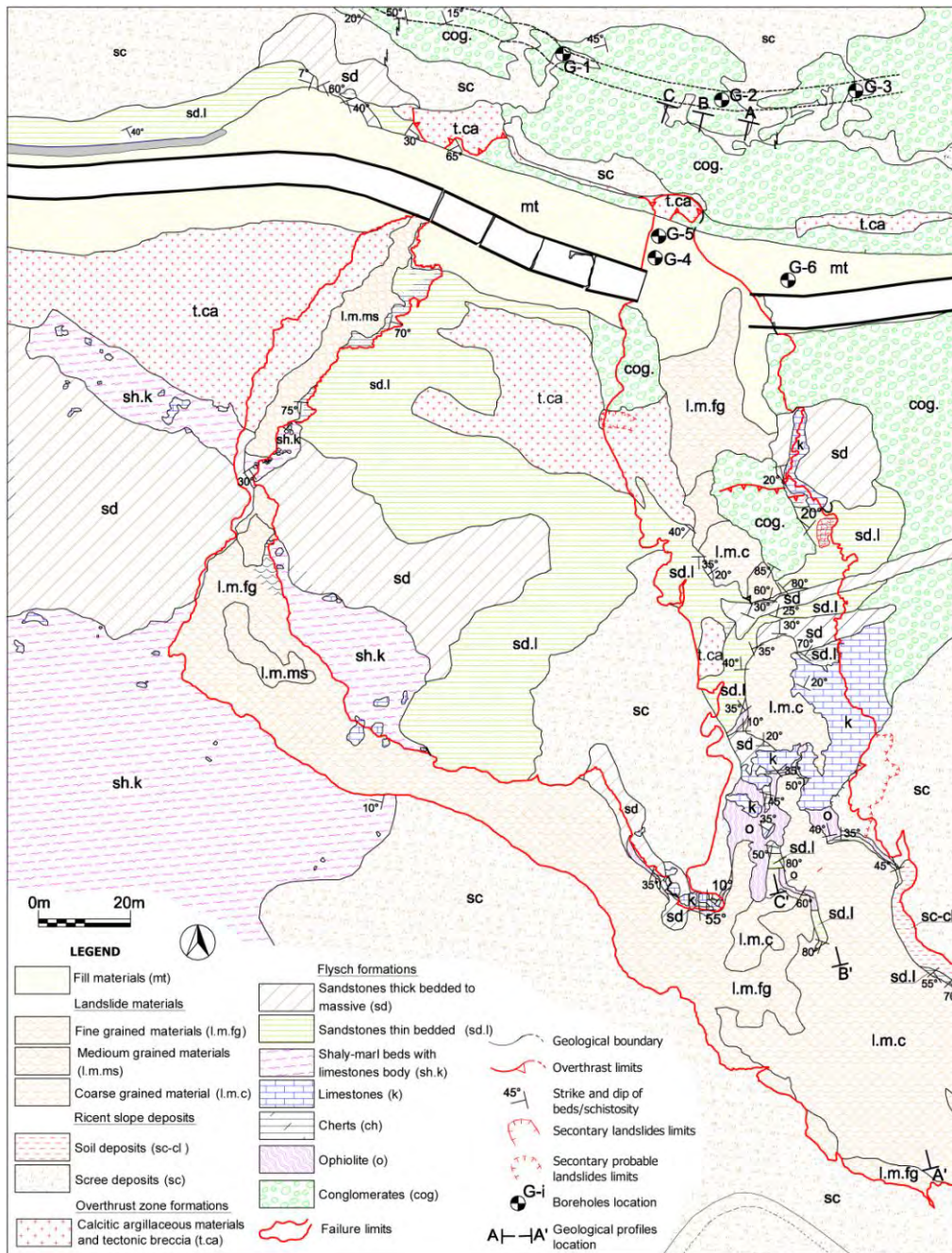
Figure 3 - Geological map of the landslide area.
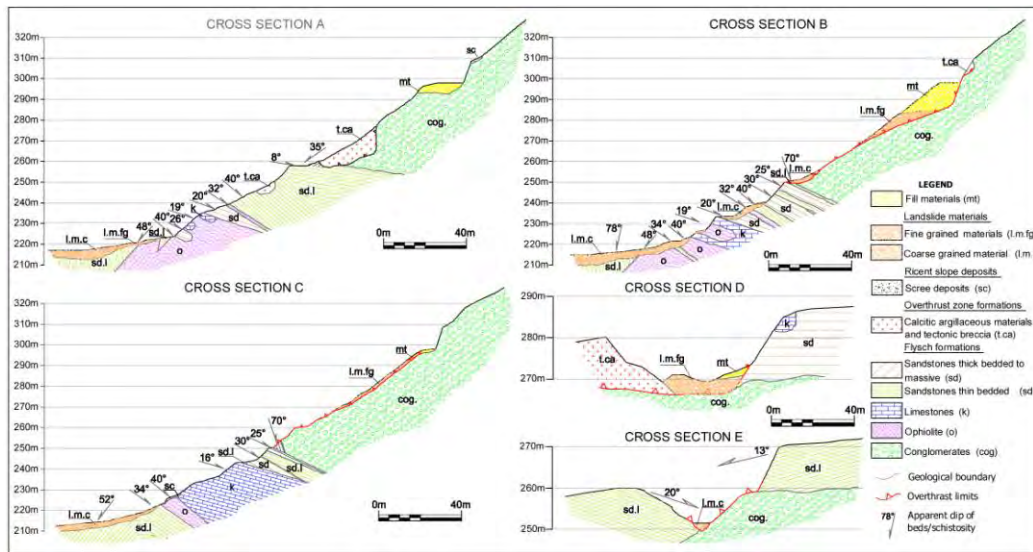
Figure 4 - Geological cross-sections of the landslide area.

5. Tectonic Structure of the Landslide Area

The north edge of the overthrust face is located along the excavated slope of the surveillance road for a length of 67m (Figures 3, 4 and 8). The overthrust surface in its western part dips 50° to 70° SW and the striations dip 55° to 70° WSW. In its eastern part, namely in the area of the main failure, the overthrust surface dips towards the SW at angles of 75° changing gradually into 35°. The soil tectonic material, which covers it, has a thickness of ca. 12 m, as determined by geotechnical borehole drillings and geophysical survey. In a distance of 50 m south of the overthrust northern edge, the surface dips 35° SSE. The striations in the overthrust plane, on the conglomerate bedrock, are dipping 50° SW. Southernmost, in a distance of 83 m from its northern edge, the last trace of the overthrust surface is located on the sandstone bedrock. The overthrust plane dips 55° SW and the striations dip 55° WSW.

The kinematic analysis of the overthrust, based on the orientation data (dip direction/dip) of the overthrust plane and the orientation of striations, revealed that this large-scale compressive event took place under a compressive stress regime of WNW-ESE direction (Figure 5).
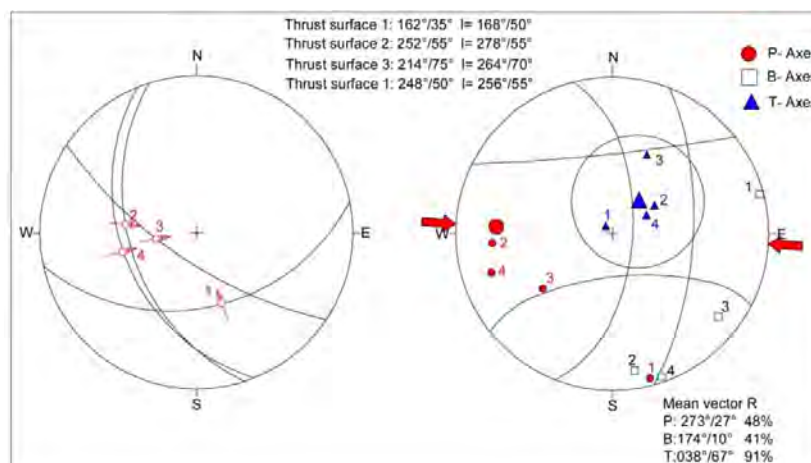
Figure 5 - Kinematic analysis of overthrust.

The tectonic depression formed in the overthrust zone was filled with calcareous-clayey, friable, light-yellow material of a thickness of 10m to 12m, as seen on the eastern slope of the eastern gully. Small-scale thrusts, with surfaces dipping mainly to the SE and ESE and secondarily to the NE at angles ranging from 30° to 35°, were mapped along the excavated slopes uphill the failure area, crossing the sandstone and conglomerate bedrock. Their length reaches 50 m, their aperture does not exceed 0.30 m and have been filled with friable calcareous-clayey material. An extended tectonic zone filled with light-yellow calcareous-clayey material, is usually formed at thrusts' ends or at their intersection (Figures 3, 4 and 8).

The rock mass is crossed by three major and one minor discontinuity sets dipping towards the SSE, NE, SW, and SE at angles ranging from 60° to 70°. According to ISRM (1981), their spacing is characterized as close to very wide (0.10 m up to 2.0 m), their persistence low (greater than 1m up to 1.50m), their surfaces are smooth to slightly rough, planar (VII–VIII), fresh with evidence of oxidation at positions, very tight to open (aperture up to 1mm), without filling material (Figure 8).

6. Investigation of the Slide Mechanism

The study of the causes of failure was based on geological mapping, evaluation of the engineering geological conditions, soil fracture characteristics, scarp geometry, the damages of the independent canal segments and their displacement, tilting and interaction, as well as the findings of the performed investigation, including geotechnical borehole drilling, inclinometers installation and geophysical survey. The evaluation outcomes regarding the causes of failure and the timeline of the failure events are presented below:

- The soil fracture and the following canal failure is not considered limited in the area of the two slid canal segments (No 6 and 7), but extended throughout the area of all the tilted canal segments (No 2 to 8). Furthermore it is delimited by the overthrust geometry. The western limit of the failure is located in the contact area of segments No 1 and 2, where a soil subsidence on the uphill side of the left canal wall is evident (Figure 6), causing tilting of segment No 2, thus enabling the canal water outflow at the right (downhill) canal wall, resulting in soil erosion and formation of the western (smaller) gully. The northern limit of the failure is related to the geometry of the overthrust.

Figure 6 - Soil subsidence on the uphill side of the left canal wall between segments 1 and 2 and along the surveillance road.

- Based on a detailed recording of the canal segments displacements (Figure 7) and their associated structural damages, it is concluded that the main displacement was perpendicular to the canal (N to S), but also along the canal with direction from segment No 2 towards segment No 5 and 6, along with rotation. The above displacement is considered to occur instantly, resulting in increase of the curvature of the canal with downhill (N to S) direction. The above

kinematics is also confirmed by the fact that all joints between hillside (northern) wall canal segments demonstrate compression failures, while all downhill (southern) wall canal segments are detached (extension).
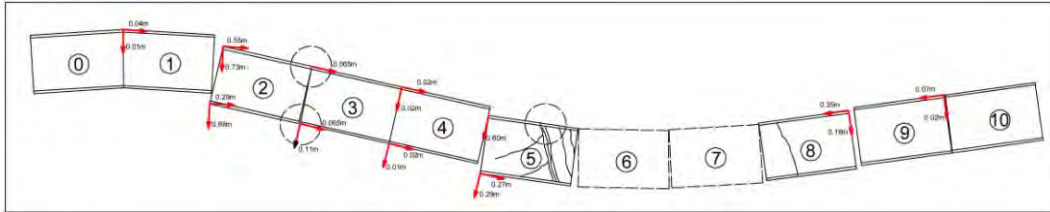
Figure 7 - Displacement of canal segments.

- With respect to the factors inducing the aforementioned displacements, groundwater hydrostatic pressure below the surveillance road, acting on the hillside (northern) canal wall, is considered critical. Based on morphology and geology of the area and the time of failure (spring time associated with high water level), it is reasonable to assume that the backfilled soil behind the hillside (northern) wall was saturated and therefore the hydrostatic pressure built up on the hillside wall and the buoyancy of the canal bottom plate, are considered as major destabilizing factors.

- The displacement of canal segments No 2 to 5 induced a void at the hillside canal wall. It is considered that this void was filled with the saturated subsoil of the surveillance road. This is demonstrated by the approximately 0.5 m vertical displacement (sinking) of the subsoil of the surveillance road in contact with the canal wall (Figure 6) and furthermore by the longitudinal cracks (parallel to the canal) on the surveillance road.

- The displacement of canal segments resulted in canal water outflow from the detached joints, which in turn caused soil erosion. The relatively large size of detachment at the joint area between canal segments No 1 and 2 resulted in severe soil erosion thus forming the western gully (Figures 1, 2). It is considered that a similar or even larger size detachment occurred at the joint area between canal segments No 6 and 7. Due to the opening of the joint between canal segments No 6 and 7, large amounts of water flowed out, causing sudden erosion and massive displacement of soil material, which finally led to the formation of the eastern gully (main slide).

- The hypothesis of a large size detachment between canal segments No 6 and 7 is considered reasonable, taking into account that the canal curvature is maximized there and furthermore due to the displacement of adjacent canal segments. Furthermore at the area of segments No 6 and 7 the thickness of erodible material (mainly tectonic breccias) is increased, thus explaining the larger size of the main slide area (eastern gully).

- With respect to the timeline of events it is considered that the canal segments displacements were practically instantaneous. The detachment of the joint between canal segments No 1 and 2, resulting in the western gully, most probably preceded the main slide, or, with less probability, both events occurred simultaneously.

7. Water-supply Remedial Works

The remedial works aimed at the restoration of the full discharge capacity of the canal, by structures founded on stable ground, delimiting any potential future hazards to the existing risk probability level of the whole canal. The decided remedial scheme included the excavation of a cut on the uphill side of the failure, where there was evidence of massive rock existence, the construction of a circular, 3.2 m diameter, bypass pipe, founded on stable rocky ground at the cut base, fully substituting the temporary, twin pipes of 2 m diameter each. Moreover, the time

margins for construction were very strict, since there was evidence that the temporary fill, where the twin bypass pipes of 2 m diameter were founded, being an immediate remedial measure, was in limit equilibrium and potentially unstable. This was suggested by its fast construction, with steep, higher that 2:3 (h:b), slope inclination, without proper compaction of the fill material of unknown grading, the creep deformations observed at the fill crown, and the readings of the inclinometer installed through the fill, which gave clear evidence of deformation.

The decided remedial works solution was based on the hypothesis of the existence of massive rock at the new cut base, suggested by the evaluation of the geological conditions and the assessment of the overthrust geometry, combined with the findings of the geotechnical investigation. These factors gave confidence on the proposed solution, which exhibits significant advantages in terms of simplicity and construction cost and time, compared to alternatives, like bypassing the failure area by a tunnel.

Based on the geological mapping of the slope faces, the quantitative description of discontinuities of the rock mass, their stereographic projection in individual rock mass parts and sliding potential failure modes, the geological structure and the engineering geological conditions along the new cut slopes, designed parallel and 5 to 6 m uphill of the existing cut, were estimated (Figures 8 and 9).
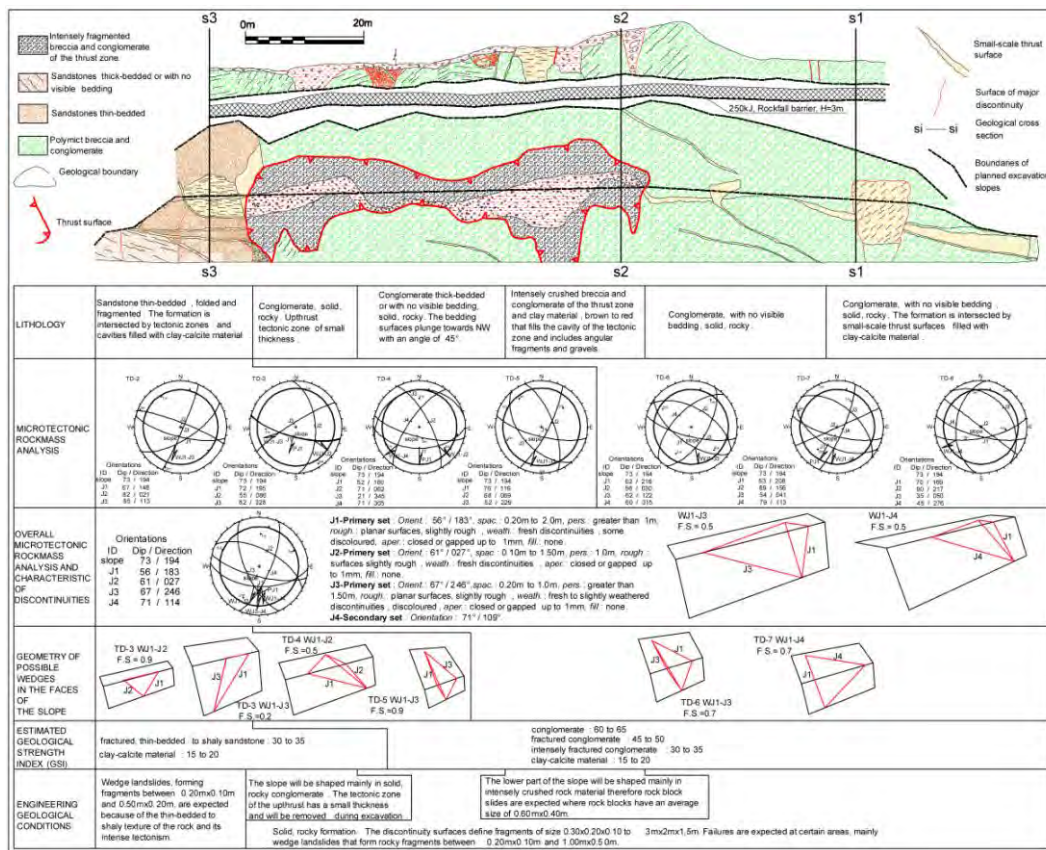
Figure 8 – Engineering geological mapping of existing slope face.

The new slope at its western end was expected to be excavated in sandstones, mainly thinly bedded and fragmented, crossed by three major discontinuity sets. Wedge failures of rock blocks of estimated sizes ranging from 0.20 m x 0.10 m to 0.50 m x 0.20 m were expected, due to the thinly bedded to foliaceous structure and intense fragmentation of the rock mass. Subsequently, the slope was anticipated to be excavated in massive to thickly bedded conglomerates, crossed by

three major and one minor discontinuity sets. Wedge failures of rock blocks of estimated size ranging from 0.20 m x 0.10 m to 1.0 m x 0.50 m, were expected. Rock quality was considered downgraded, mainly in the overthrust area and also in places where the rock mass was crossed by small-scale thrusts and major joints. The development of small-scale cavities filled with clayey and calcareous-clayey material was considered possible (Figures 8 and 9).
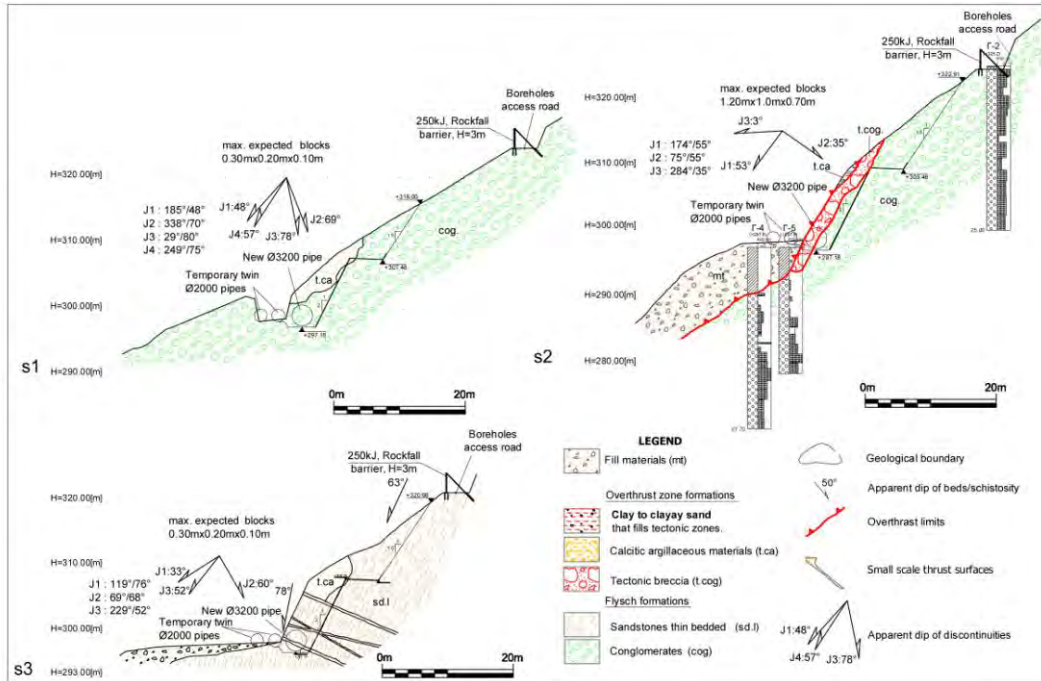
Figure 9 – Engineering geological cross-sections along the new slope.

The average cut height was 25 m. The cut was excavated mostly within fresh and massive rock, as expected. A 5 m wide berm was constructed at intermediate height of the cut, for stability and protection reasons. The cut inclination was selected 2:1 (h:b) below the berm and 3:2 (h:b) above it. Stability measures included installation of 6 m long rockbolts of 200 kN capacity in 3 m x 3 m pattern, and application of wire mesh on the upper part of the slope and wire mesh combined with 10 cm shotcrete on the lower part of the slope. To ensure protection against rockfalls commencing on the natural slope above the cut, the construction of a 3m high rockfall barrier, of 250 kJ capacity at the cut crown, in front of a rock trap, was constructed. Finally to avoid water pressures behind the shotcrete, installation of a row of drainage holes of 3'' diameter was also implemented (Figure 10).

8. Rehabilitation of the Slide Area

The safe restoration of the canal water supply, being urgent and critical, has been achieved, though the completion of the remediation should include also rehabilitation of the slide area. The proposed solution for the rehabilitation comprises the removal of the southern temporary pipe of 2 m diameter, in order to provide space at the crest of the temporary fill, for the construction of a pile wall, of 80 cm diameter concrete piles. The pile wall will secure the stability of the remaining northern temporary pipe of 2 m diameter and will be used as temporary support for the suggested excavation in order to remove the loose temporary fill. Excavation of the loose fill will be executed in stages and the pile wall will be supported by two rows of pre-stressed anchors (Figure 11).
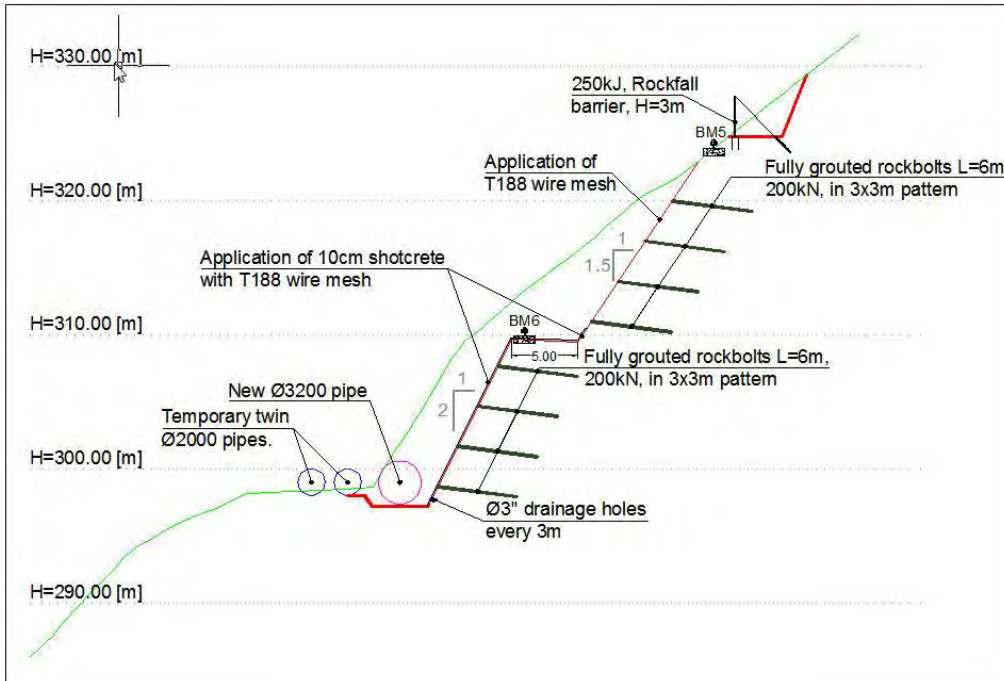
Figure 10 – Excavation geometry - support and protection measures.
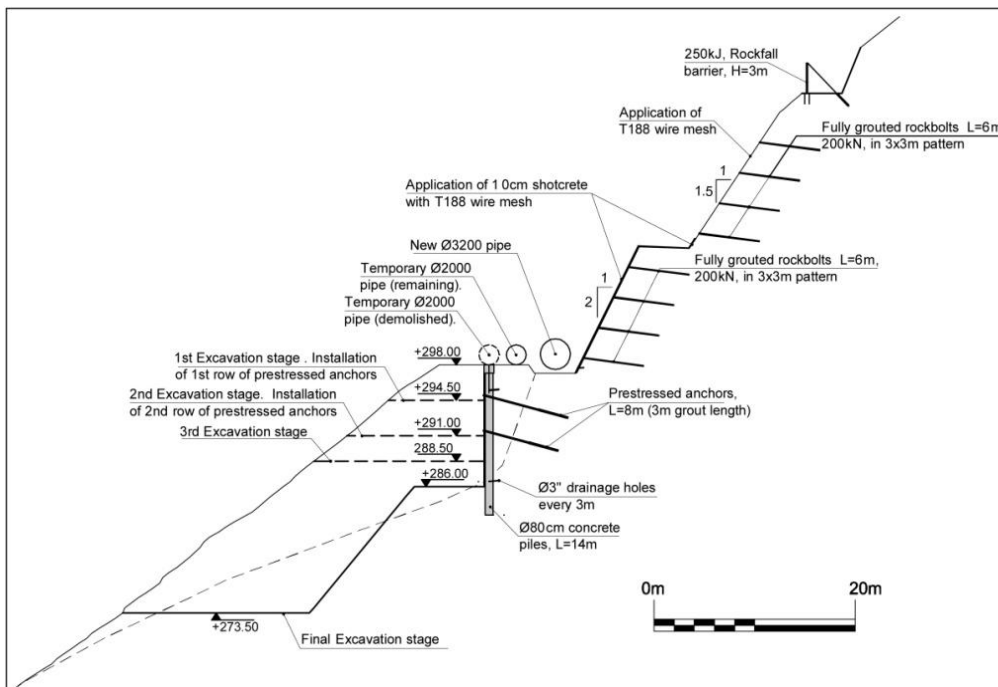
Figure 11 - Support measures and excavation stages for removal of temporary fill.

Following the above construction methodology, full removal of the uncompacted temporary fill or any other loose superficial material is feasible. Rehabilitation will be achieved by the construction of a reinforced embankment under fully controlled conditions, founded on sound rock (Figure 12).
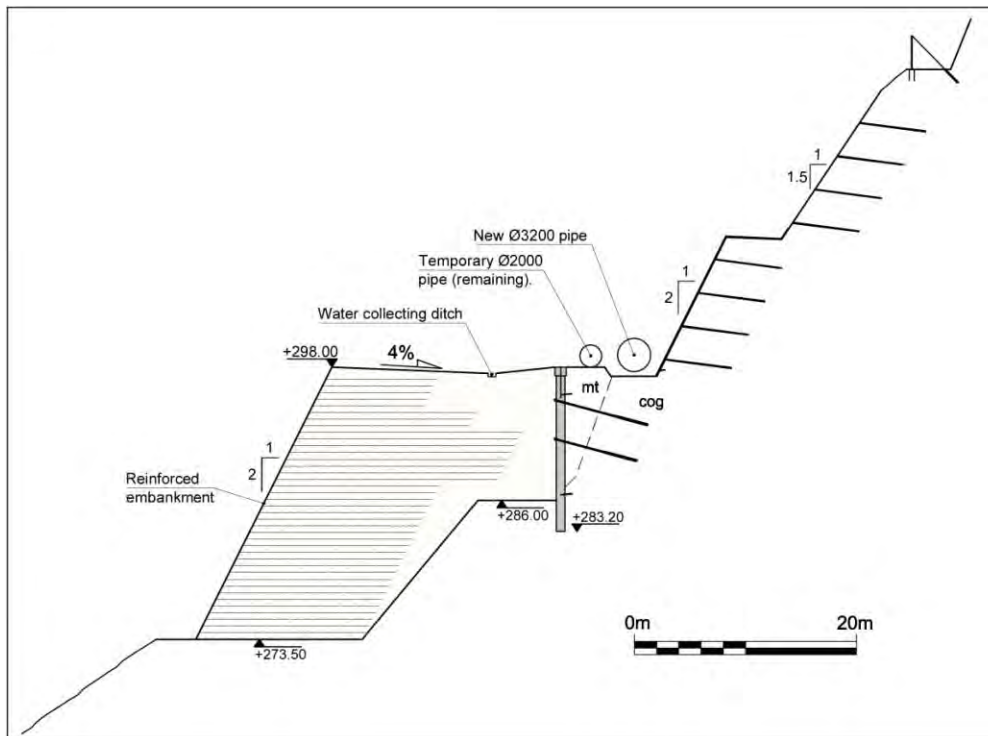
Figure 12 - Rehabilitation by reinforced embankment construction.

9. Design Implementation

The proposed cut was excavated from February to August 2012. The encountered geological conditions fully complied with the expected ones and the application of the proposed stability and protection measures ensured long term stability. Furthermore, construction of the new by-pass pipe of 3.2m diameter, founded on sound rock, was completed by September 2012 and its operation commenced in November 2012. Pile wall construction is expected to commence in spring 2013 and will be followed by the slide rehabilitation by means of the proposed reinforced embankment.

10. Acknowledgements

11. References

Anderson S.A. and Sitar N. 1995. Analysis of rainfall-induced debris flows, *J. Geotech. Eng.,* 121, 544-552.

Berti M., Genevoi R., Simoni A. and Tecca P.R. 1999. Field observations of a debris flow event in the Dolomites, *Geomorphology*, 29, 265-214.

Berti M. and Simoni A. 2005. Experimental evidences and numerical modeling of debris flow initiated by channel runoff, *Landslides,* 2, 111-182.

Bovis M.J. and Dagg B.R. 1992. Debris flow triggering by impulsive loading: mechanical modeling and case studies, *Canadian Geotechnical Journal*, 29, 345-352.

Bovis M.J. and Jakob M. 1999. The role of debris supply conditions in predicting debris flow activity *Earth Surface Processes and Landforms*, 24, 1039-1054.

Cannon S.H., Bigio E.R. and Mine E. 2001a. A process for fire-related debris flow initiation, Cerro Grande fire, New Mexico, *Hydrological Processes*, 15, 3011-3023.

Cannon S.H., Kirkham R.M. and Parise M. 2001b. Wildfire-related debris flow initiation processes, Storm King Mountain, Colorado, *Geomorphology*, 39, 111-188.

Cannon S.H., Gartner J.E., Parrett C. and Parise M. 2003. Wildfire related debris-flow generation through episodic progressive sediment-bulking processes, western USA. In: Rickemann, D., Chen, C.L. (eds), Debris-Flow Hazards Mitigation - Mechanics, Prediction and Assessment, *Proc. of the 3rd International Conference on Debris-Flow Hazards Mitigation*, 10-12 September 2003, I, 71-82.

Cenderelli, D.A. and Kite, J.S. 1998. Geomorphic effects of large debris flows on channel morphology at North Fork Mountain, eastern West Virginia, USA, *Earth Surface Processes and Landforms*, 23, 1-19.

Coe J.A., Kinner D.A. and Godt J.W. 2008. Initiation conditions for debris flows generated by runoff at Chalk Cliffs, central Colorado, *Geomorphology*, 96, 210-297.

Dadson S.J., Hovius N., Chen H., Dade B.W., Lin J.C., Hsu M.L., Lin C.W., Horng M.J., Chen, T.C., Milliman J. and Stark C.P. 2004. Earthquake-triggered increase in sediment delivery from an active mountain belt, *Geology*, 32, 733-736.

Egashira S., Honda N. and Itoh T. 2001. Experimental study on the entrainment of bed material into debris flow, *Physics and Chemistry of the Earth (C),* 26, 9, 645-650.

Godt J.W. and Coe J.A. 2007. Alpine debris flows triggered by a 28 July 1999 thunderstorm in the central Front Range, Colorado, *Geomorphology*, 84, 1-2, 80-97.

Hungr O., McDougall S. and Bovis M. 2005. Entrainment of material by debris flows. ln Jakob, M., Hungr, O. (eds) *Debris-flow hazards and related phenomena*, Springer Berlin, Heidelberg, 135-158.

ISRM Suggested Methods 1981. In Brown, E.T. (ed), *Rock Characterization Testing & Monitoring*, Pergamon Press, 211pp.

Iverson R.M., Reid M.E. and LaHusen R.G. 1997. Debris flow mobilization from landslides, *Annu. Rev. Earth Planet. Sci.,* 25, 85-138.

Jakob M., Bovis M. and Oden M., 2005. The significance of channel recharge rates for estimating debris-flow magnitude and frequency, *Earth Surface Processes and Landforms*, 30, 155-166.

Keefer D.K. 1984. Landslides caused by earthquakes, *Geological Society of America Bulletin*, 95, 4, 406-421.

Leonards A.G. Sotiropoulos, E.S. Mourtzas N.D., Marinos P.G. and Kountouris P.J. 1993. Two case studies of slope instability in soft rock, in Anagnostopoulos et al. (eds), *Geotechnical Engineering of Hard Soils-Soft Rocks*, Balkema, Rottetdam, 1125-1136.

Major J. 2000. Gravity driven consolidation of granular slurries: implications for debris-flow deposition and deposit characteristics, *Journal of Sedimentary Research*, 70, 1, 64-83.

McCardell B.W., Bartelt P. and Kowalski J. 2007. Field observations of basal forces and fluid pore pressure in a debris flow, *Geophysical Research Letters*, 34*,* L07406, doi: 10.1029/2006GL029183.

McCoy S.W., Kean J.W., Coe J.A., Staley D.M., Wasklewicz T.A. and Tucker G.E. 2010. Evolution of a natural debris flow: In situ measurements of flow dynamics, video imagery and terrestrial laser scanning, *Geology*, 38, 8, 735-738.

Papanikolaou D. 1986. Geology of Greece, Eptalofos Publications, Athens, 240pp.

Papastamatiou I., Tataris A.A., Maragoudakis N. and Monopolis D. 1971. Geological map of Greece: Levadia sheet (scale 1:50.000), IGME Publications, Athens.

Santi P.M., deWolfe V.G., Higgins J.D., Cannon S.H. and Gartner J.E. 2008. Sources of debris flow material in burned areas, *Geomorphology*, 96, 310-321.